ISSN: 2639-7455

Research Article

Earth & Environmental Science Research & Reviews

Proterozoic Slushball Earth and Generation of Excess Oxygen not achieved by Photosynthesis

Mikio Fukuhara*[1], Ken'nosuké Hara [2]

[1]*New Industry Creation Hatchery Center, Tohoku University, Sendai, Japan 980-8579*

[2]*Sendai 982-0252, Japan*

***Corresponding Author**
Mikio Fukuhara, New Industry Creation Hatchery Center, Tohoku University, Sendai, Japan.

Submitted: 2023, Apr 20; **Accepted**: 2023, May 29; **Published**: 2023, June 20

Citation: Fukuhara, M., Hara, K. N. (2023). Proterozoic Slushball Earth and Generation of Excess Oxygen not achieved by Photosynthesis. *Eart & Envi Scie Res & Rev, 6*(3), 497-507.

Abstract

According to the Earth-scale top model, the Earth's axis was tilted approximately 1.8 billion years between 2.7 billion to 900 million years ago. This resulted in the freezing of the equatorial zone and the recognition of a Slushball Earth, explaining the Pongola, Huronian, Sturtian, Marinoan, and Gondwana -glaciations as well as numerous other historical events of the Earth. The hypothesis that nitrogen, oxygen, and water were formed due to nuclear transmutation at high temperatures and pressures, suggests that excess oxygen was produced during photosynthesis and nitrogen and water were expelled into the atmosphere from magma reservoirs in the upper mantle through an open system which caused volcanoes in ocean islands. The evolution of atmospheric oxygen concentration leading to the development of life over the past 400 million years, can be explained by the nitrogen released into the stratosphere through open systems while the magma reservoirs are blocked.

Introduction

Since Earth's formation, it has experienced several periods of cold weather, known as glacial period or glaciation. The oldest known ice age is the Pongola, which occurred in South Africa approximately 2.9 billion years ago, while the most recent is the Late Cenozoic ice age, which continues to this day [1]. Following Harland's theories [2] regarding Neoproterozoic glaciers, the "Snowball Earth" hypothesis was first proposed by Salyards et al. [3]. Then, Hoffman et al. [4] summarized the results of a cap carbonate survey in Namibia, South Africa, in the so-called "global freezing" hypothesis. The Snowball Earth hypothesis asserts that the entire Earth was completely covered in ice sheets and sea ice, including near the equator, in the last stage of the early Proterozoic Huronian Ice Age (2.45–2.2 billion years ago) and the Late Proterozoic Sturtian and Marinoan Ice Ages (730–635 million years ago). Proponents of this theory have challenged the geological evidence for global glaciation and the geophysical feasibility of ice- and mud-covered oceans [5, 6] and have emphasized the difficulty of escaping a total freeze. Many questions remain with regards to this hypothesis, including whether the Earth was either a perfect snowball or a "slushball" with a thin equatorial open water zone (or seasonally open water zone) [7]. A competing hypothesis to explain the presence of ice on the equatorial continents is based around the Earth's axial tilt angle being approximately 90°. Williams reported a high-obliquity low-latitude ice and strong seasonality (HOLIST) hypothesis based on a large inclination in the Earth's axis [8]. However, his hypothesis has been refuted because of its mechanical difficulty [3], and scarce supporting evidence [4].

Hara [9] proposed another explanation for the phenomenon of low-latitude glaciation based on Earth-scale top model, that is, an extended period of time in a sideways inclination over 1.8 billion years from about 0.9 to 2.7 billion years ago at an axis of rotation tilt angle θ ~90°, which would result in weak sunlight over the equatorial zone, resulting in a long-running susceptibility to freezing. This alternative to the Snowball Earth hypothesis is the so-called "Slushball Earth" hypothesis. Ice entombed events are believed to have caused the mass extinction of protists, known as the Great Extinction, and the subsequent leap in biological evolution, known as the Cambrian Explosion. The emergence of oxygen-breathing organisms and multicellular organisms, known as the Ediacaran biota are thought to be closely related to ice-entombed events. Our interests lie in the Slushball Earth hypothesis and the generation of excess oxygen during glacial periods, from 2.7 billion years ago to present. Due to the unavailability of directly observed astrophysical and geophysical data to explain the variations in the axial tilt of the Earth system model and the formation of oxygen, respectively, these questions need to be analyzed using circumstantial evidence and insights gained into

Earth's historical events using other types of data.

Neoproterozoic Slushball Earth

The evolution of the tilt angle of the Earth has greatly influenced its dynamic, climatic, and biotic development. Williams first proposed this possibility based on the normal climatic zonation during the Phanerozoic, the paradoxical Late Proterozoic glacial climate, the seeming reserve climatic zonation of the Precambrian in general, and the single giant impact hypothesis for the origin of the Moon [10]. Because he did not show the precise variation of Earth's obliquity over its history, the variation in the obliquity was thought to be impossible.

Hara [9] proposed another explanation for the phenomenon of low-latitude glaciation based on Earth-scale top model, that is, an extended period of time in a sideways inclination over 1.8 billion years. This model simulated the change in the inclination of the spin axis of Earth after starting at $\theta = 179.5^{\circ}$ provided that actual real-Earth values $(C\text{-}A)/C = 0.0034$ and $\omega = 366.25\ \Omega$ (365.25 spins about its axis a year and one geometric spin generated by one revolution around the Sun [111]), based on the well-known precession-nutation theory with the hypothetical gyroscope-effect, where θ is the direction of an axial tilt angle from the north ecliptic pole, C and A are moments of inertia along and transverse to the axis of symmetry, respectively; ω and Ω are spin and revolution rates, respectively (Appendix 1). Figure 1 shows the reversing motion of the symmetry axis of the Earth-scale top from 4.6 billion years ago to the present time, along with various geophysical and biological events in Earth's history. This curve is distinct over a long time-interval (1.8 billion years) of sideways tilt ($\theta \approx 90^{\circ}$) from 2.7 to 0.9 billion years ago, corresponding to low-latitude glaciation.

From the results of a cap carbonate survey in Namibia, Hoffman et al. [4] reported that the "global freezing" hypothesis explains many extraordinary observations in the geologic record of the Neoproterozoic world: (1) the presence of striated iron deposits; (2) evidence of long-lived glaciers at sea level in the tropics; (3) mystery of the presence of cap carbonate rocks; (4) Carbon isotope changes associated with glacial deposits. Since Hoffman et al. refuted Jenkins' and Scotese's thesis [12] with four striking features of late Proterozoic glacial deposits, here, we will attempt to answer four questions, taking the Proterozoic Slushball Earth hypothesis into consideration.

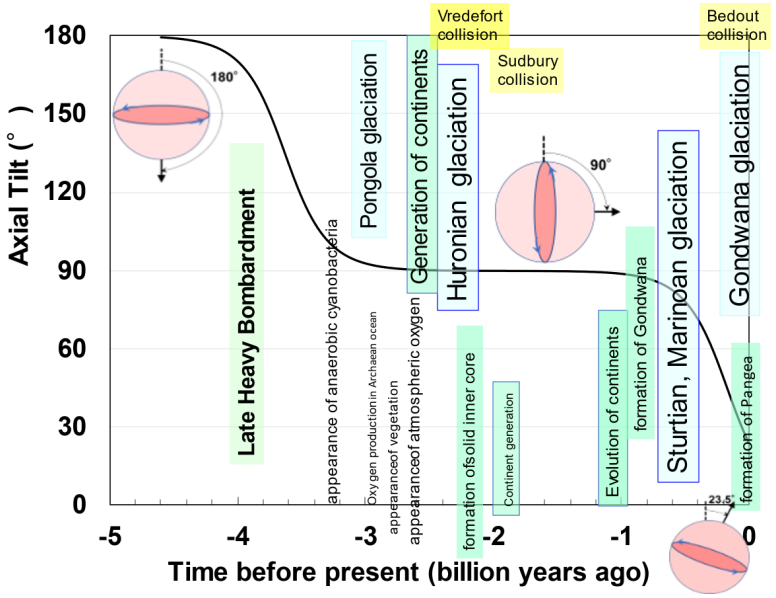

Figure 1: Changes in the axial tilt of Earth from billions years ago to the present time, along with historical geoscientific events. Earth with different axial tilts (180°, 90°, and 23.5°). ttps://doi.org/10.1038/scientificamerican0509-36.

1. Presence of striated iron deposits

Striped iron ores are alternating accumulations of iron oxide-rich and silica-rich layers, and are widely distributed throughout the world, including special Australia and Brazil. This deposit is known to have formed in large quantities approximately 2.5 to 2 billion years ago [13, 14]. This indicates that the ice-covered oceans were anoxic because gas exchange with the atmosphere was blocked, and divalent iron ions were dissolved under anoxic conditions. Since continental formation began in the early Proterozoic, and by the late Proterozoic the Rodinia supercontinent assembled near the equator [15], the formation of striated iron ores can be explained by the freezing of equatorial regions associated with Earth's tilting (Fig. 1). However, the fact that few striated iron ores have formed since their formation approximately 1.8 billion years ago implies that the oxygen concentration in the atmosphere has increased to some extent, as illustrated in Fig. 2. On the other hand, the striated iron ore deposits in the Late Proterozoic, which have not formed in a billion years, are thought to have formed again because magmatic activity caused the supply of reducing materials from the submarine hydrothermal system, resulting in a hypoxic environment [3].

2. Paleomagnetic Evidence of the Existence of Continental Ice Sheets in Equatorial Regions

When sedimentary rocks form, the magnetic minerals within them tend to coincide with the Earth's magnetic field. As a result, paleomagnetism can be used to estimate the latitude at which the rocks were deposited. The paleomagnetic position of glacier-derived deposits (e.g., dropstones) suggests that glaciers extended from land to sea level at tropical latitudes at the time that they were deposited [16]. Currently, the only sediments known to have been deposited at low latitudes are the Elatina sediments of Australia, whose depositional age is well constrained and the signal is clearly original [17]. Based on the magnetic orientation of tiny mineral grains in glacial sediments, Harland asserted that all continents had assembled near the equator in the Neoproterozoic [2]. The long-lived sideways tilt ($\theta \approx 90°$) for 1.7 billion years in Fig. 1 explains how glaciers could have survived tropical heat.

3. Existence of Cap Carbonates in Neoproterozoic Glacial Times

Neoproterozoic glacial deposits are blanketed almost everywhere by carbonate rocks [4].The existence of cap carbonates indicates that carbonates were abruptly formed in warm, shallow seas due to sudden climate change after the glaciers dropped their last loads. This is because a decrease in the axis of rotation inevitably raises temperatures and melts glaciers in equatorial regions. The thick sequences of carbonate rock are the expected consequence of global warming unique to the transient aftermath of the Slushball Earth, corresponding to recovery from a 90° tilt of the axis of rotation starting at approximately 900 million years ago.

4. Carbon isotopic variations

Carbon isotope ratios ($^{13}C/^{12}C$) show anomalously large values (~10‰) below the glacial deposits, but which begin to decline just before the glacial deposits, dropping to values of -6 ‰ in the immediate vicinity of the glacial deposits [3]. This value is that of volcanic gases supplied to the atmosphere and ocean. This negative anomaly in carbon isotope ratios suggests an almost complete cessation of photosynthetic activity by organisms shortly after the glacial period, (*i.e.*, the Great Extinction of life 0.44 billion years ago (late Ordovician period) and 0.36 billion years ago (late Devonian) [18], corresponding to 74.2° and 67.5° respectively).

However, there are several problems with designating a glacial origin for cap carbonate [19]: (1) dissolution of carbonates owing to ocean acidity when carbon dioxide concentrations are high; (2) the uncertain existence of cap carbonate.

Considering the Slushball Earth hypothesis, a number of mechanisms have been reported for the onset of frozen Earth, including supervolcano eruptions, reduced atmospheric concentrations of greenhouse gases, such as methane and carbon dioxide and changes in solar energy output. Regardless of the trigger, the initial cooling may have eventually frozen the equator as cold as modern Antarctica owing to the reflection of solar energy back into space (increased Earth albedo) caused by the increased surface area of the Earth covered in ice and snow. Furthermore, the positive feedback would have cooled the Earth further.

Although the existence of glaciers is not disputed, the idea that the entire planet was covered in ice is disputed. Some scientists therefore postulate the "Slushball Earth", in where sediments are only formed in open water or under rapidly moving ice, or where the hydrological cycle continued in thin ice-covered waters [7]. Computer modelling using energy balance and general circulation models suggests that large areas of the ocean should have remained ice-free and argues that "hard" snowballs are not plausible [20].

A theory that neatly explains the Slushball Earth hypothesis is the overturning of the Earth's axis hypothesis, as proposed by Hara [9], which spans a period of 1.8 billion years elapsed from about 2.7 to 0.9 billion years ago. As shown in Fig. 1, the emergence of anaerobic cyanobacteria, Pongola glaciation, generation of oxygen in the oceans, generation of plants, and generation of atmospheric oxygen occurred before the 90° axis rotation of Earth; whereas, the onset of continental development, Hugo-Anglian glaciation, formation of the solid inner core, formation of continents in the equatorial region, and the development of continents after the formation of the Gondwana supercontinent occurred during the 90° tilt. The Earth's axial tilt began to gradually decrease, accompanied by the Sturtian and Marinoan glacial periods. With the evolution of the Pangaea supercontinent, the Gondwana ice age arrived, leading to the present-day axial ratio of 23.5°.

The glaciers began to recede around 900 million years ago due to a decrease in the tilt of the Earth's axis and a higher concentration of carbon dioxide in volcanic gases and methane gas in the atmosphere due to global warming, followed by a further decrease in temperature due to the weathering of rocks and re-dissolution of carbon dioxide and methane gases into the ocean, resulting in the Sturchian glaciation, followed by the Marinoan and Gaskiers glaciations. However, as the major glacial episodes ended millions of years before the Cambrian explosion, there were three or four smaller glacial periods during the Late Neogene because of these icehouse–greenhouse cycles. When ice melted on Slushball Earth, freshwater layers on land and ocean surfaces provided many new opportunities for biological evolution.

Generation of excess oxygen unachieved by photosynthesis

Oxygen gas plays a major role in driving evolution, associated with both the dramatic development of life and mass extinctions. Here, we note the generation of excess oxygen not achieved by photosynthetic reactions on Slushball Earth. Change in O_2 concentrations can be divided into three time periods [21, 22, 23]: very low content before 2 billion years, rapid accumulation (popularly known as "Great Oxidation Event" (GOE) [22] in the Precambrian era from 2 to 0.42 billion years ago, and saturation content from 0.42 billion years ago to the present time. The results are summarized in Fig. 2. We can find three-time period (3.0, 1.9 and 0.8 billion years ago) enhancements for the great oxidation event. The formation of a small amount of free O_2 on the sea surface by ultraviolet photochemical reactions [24] in the Archean era can be expressed as:

$$2H_2O + 4h\nu \rightarrow 4e^- + 4H^+ + O_2 \qquad (1)$$

According to the present consensus [25], oxygen gas was generated as a result of photosynthetic activity. After the first oxygenic photosynthesis by anaerobic cyanobacteria from 3.5 billion years onward, aerobic photosynthesis by plants, algae, and cyanobacteria (eubacteria) produced oxygen gas and carbohydrates from H_2O and CO_2 since 2.7 billion years ago. Photosynthetic reactions can be represented by a single well

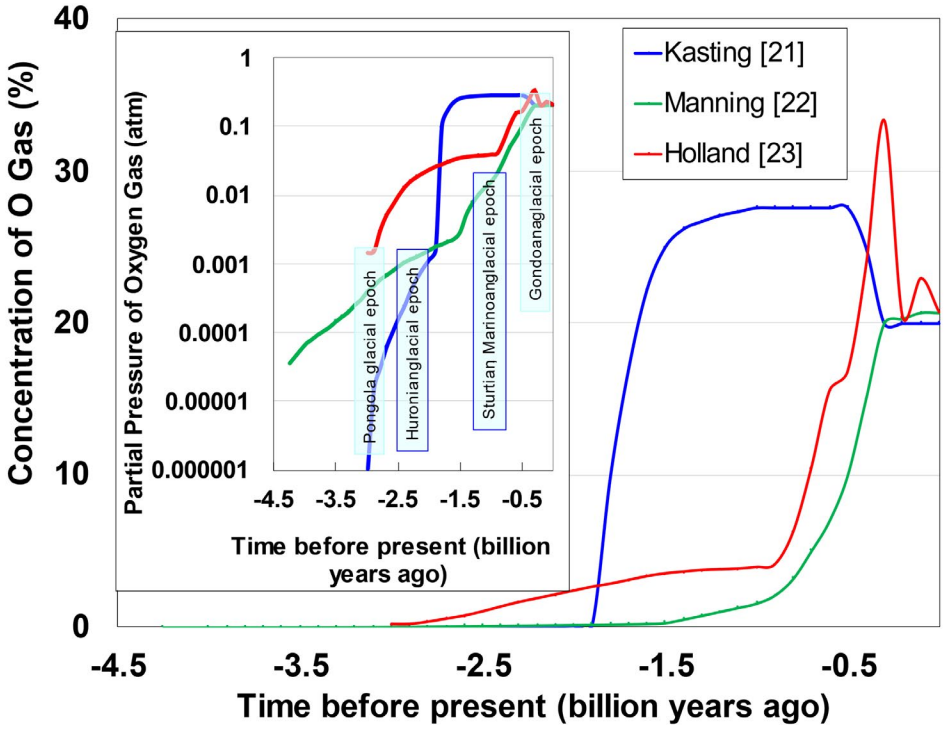

Figure 2: Changes in concentration of atmospheric O_2 from 4.5 billion years ago to the present time, using data obtained by three researchers [21-23]. The inset shows a logarithmic plot of partial pressure of O_2 gas against time since 4.5 billion years ago. Four representative glacial periods correspond to rapid increases in partial pressure of oxygen gas.

recognized formula given by Eq. (2) [26]:

$6CO_2 + 6H_2O$ + light energy (2,870 kJ/mol) → $C_6H_{12}O_6$ (glucose) + $6O_2$. (2)

It is known that 1 mol of CO_2 produces 1 mol of O_2 from Eq. (2). In other words, the volume of the reaction did not vary. Therefore, the rapid increase in oxygen gas since 2 billion years ago cannot be explained solely by photosynthesis because the absolute amount of carbon dioxide is too small [27].

Fukuhara proposed a model for the formation of nitrogen, oxygen, and water using circumstantial evidence based on the history of Earth's atmosphere [27, 28]. This hypothesis suggests that endothermic nuclear transformation changes the carbon and oxygen nuclei confined in the aragonite ($CaCO_3$) lattice in magma reservoirs into nitrogen and helium nuclei. Nuclear transformation is enhanced by the attraction caused by high temperatures (≥ 2510 K) and pressures (≥ 58 GPa) in the upper mantle. We obtained Eq. (3) for the completely closed system by the subsequent reactions with photons (γ) and neutrons (n), as shown in Appendix 2:

$2^{12}C + 2^{16}O + 4e^* + 4\bar{\nu}_e + 2\gamma \rightarrow {}^{14}N_2\uparrow + 1/2{}^{16}O_2\uparrow + {}^{1}H_2{}^{16}O\uparrow + 2n$ -10.58 MeV (3)

When we focus on igneous gases in magma reservoirs in the upper mantle, we see that the nuclear transformation is under open systems with lids, such as magma materials released into the atmosphere, holding high temperatures and pressures (Fig. 3), because of a depth of over 600 km. Here we define the mean blockade of craters as $0 \leqq \bar{x} \leqq 1$, as follows:

$$\bar{x} = \sum_{i=1}^{n} x_i\,(T)/n, \quad (4)$$

where $x_i\,(T)$ is the blockade degree exhibited by the i-th ocean-island-type volcano during a certain period T. Strictly speaking, the right-hand term of Eq. (A19) in Appendix 2 is first separated into two parts, $(1-\bar{x})$ $(2^{14}N + {}^4He)$ and $\bar{x}$ $(2^{14}N + {}^4He)$, when $\bar{x} \neq 1$, and the successive nuclear reactions shown in Appendix 2, Eqs. (A20) –(A23) are only applied to the latter. Thus, we obtain:

$4^{12}C+4^{16}O+8e^*+8\bar{\nu}_e + 4\,\bar{x}\,\gamma \rightarrow 4(1-\bar{x})^{14}N_2\uparrow+4(1-\bar{x})^{4}He\uparrow+2\,\bar{x}\,{}^{14}N_2\uparrow+\bar{x}\,{}^{16}O_2\uparrow+2\bar{x}\,{}^{1}H_2{}^{16}O\uparrow+4\bar{x}n$ (5)

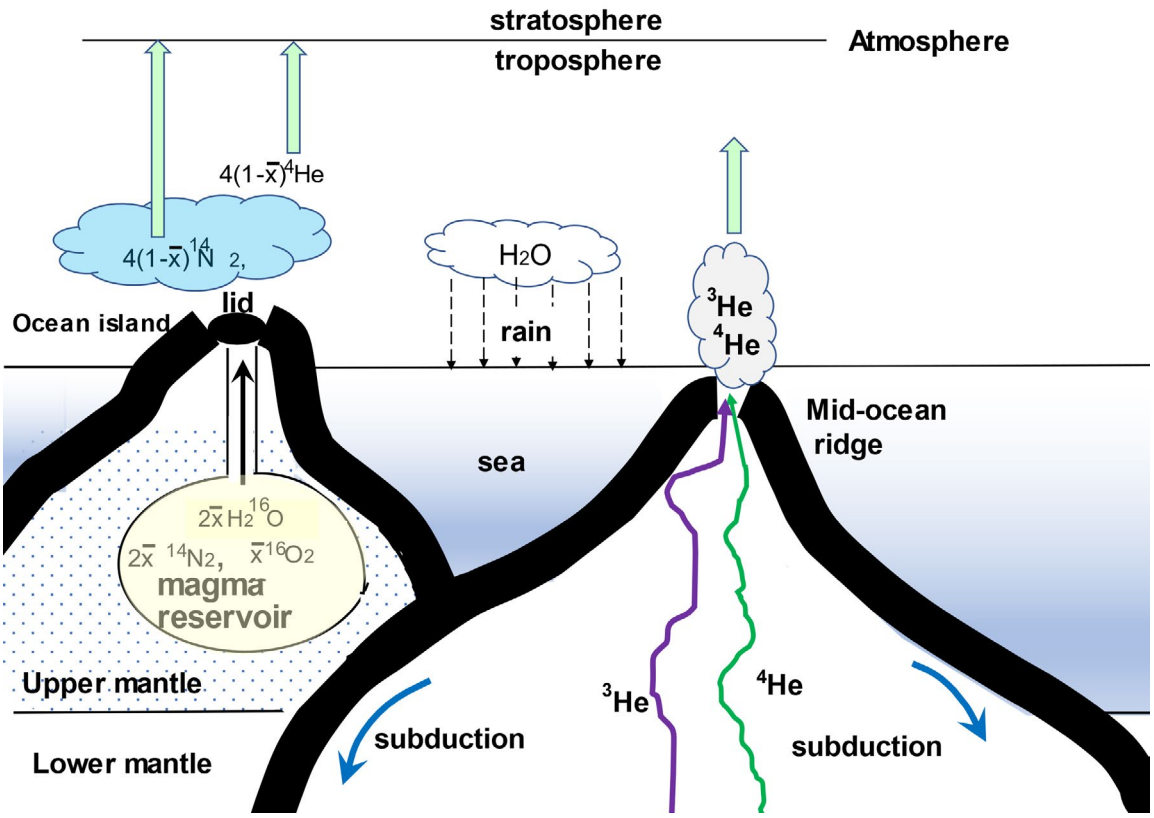

Figure 3: Schematic illustration of nuclei transformations in a magma reservoir of an ocean island and a Mid-ocean ridge. N_2, O_2, and H_2O are produced in the magma reservoir in the upper mantle, and ^3He and ^4He are formed from reservoirs of the lower mantle.

As water vapor circulates in the atmosphere to form rain and He gas is easily released from the troposphere into the stratosphere, we only consider atmospheric nitrogen and oxygen.

The following equation is obtained as the concentration of oxygen gas X from the right- hand term in Eq. (5) ($O_2/N_2 = \bar{x}/2(2-\bar{x})$, therefore:

$$X = \bar{x} / (4- \delta - \bar{x}), \qquad (6)$$

where δ is the nitrogen released into the stratosphere when the magma reservoirs are blocked. The causes of the blockade are considered to be the sealing of craters by tenacious lava and thick frozen snow (or ice). Figure 3 provides a schematic illustration of the formation of $2\bar{x}$ mol nitrogen and $\bar{x}$ mol oxygen in the magma reservoir of the upper mantle and $4(1-\bar{x})$ mol nitrogen in the atmosphere by an open system with a mean blockade $\bar{x}$. While ^3He and ^4He are produced by two- and three-body nuclear fusions, respectively, of deuterons confirmed in hexagonal FeDx core-center crystals, since they are released from mid-ocean ridge islands derived from the proto-plume such as Baffin and West Greenland Islands [29, 30] through the lower mantle [31]. In this study, we only considered nitrogen and oxygen interacting with the troposphere. We calculated the oxygen concentrations using Ward's atmospheric oxygen concentrations over the last 400 million years [32]. The results of which are shown in Fig. 4. The maximum oxygen concentration did not exceed 30% over 400 million years to date. In the inset of Fig. 4, the curves of oxygen concentration versus mean blockade are shown as functions when the values of δ are 0, 1, 2 and 2.7 (Eq. (6)) over 400 million years. Surprisingly, the oxygen concentrations over 400 million years (Ward's data [30]) were approximately expressed as a function of the mean blockade when δ was 2.7. This indicates that the amount of nitrogen gas released into the stratosphere has been constant over 400 million years and the percentages of the release, $100\ \delta/ (4-2\ \bar{x})$, are 76±3% using the relation that $\bar{x} = 0.14 – 0.30$ for X=12 – 30% which are obtained from a curve corresponding to δ =2.7 (Fig.4, inset). The value of 76% is less than the well-known value of helium gas release 84% [27, 31]. These results indicate that the reaction in the volcano was open. The fact that the present oxygen concentration of 20.8% corresponds to the mean blockade of magma reservoirs, $\bar{x} = 0.27$ (Fig. 4, inset), is very suggestive in view of volcanic activity. Basalt is less viscous but tends to cap volcanoes, as well as freeze. This is reasonable because the cover of the craters must be opened periodically.

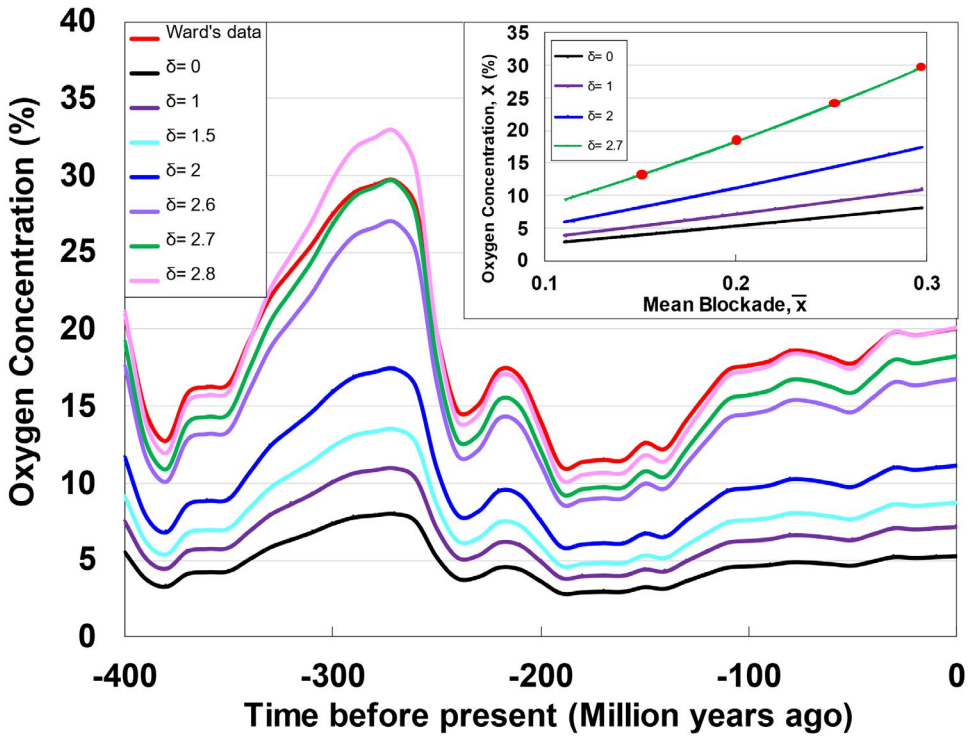

Figure 4: Relationship between atmospheric oxygen concentration, X, and nitrogen gas portion δ released into the stratosphere over the last 400 million years, which are obtained using a computational technique. Inset: Relationship between oxygen concentration, X, and the mean blockade of magma reservoirs, ($\bar{x}$), when δ=0, 1, 2, and 2.7. Four red closed circle are obtained from Eq. (7) at the values of δ=3 and α=0.27.

The above results are those when only the nitrogen gas release was considered and we introduce briefly a trial that the oxygen gas release is simultaneously considered.

A model that the loss of oxygen is proportional to α times the molar volume ratio of oxygen to nitrogen gases is shown in Eq. (7):

$$X = \frac{\bar{x} - \alpha\left(\frac{\bar{x}}{4-2\bar{x}}\right)\delta}{4-\delta-\bar{x}+\alpha\left(\frac{\bar{x}}{4-2\bar{x}}\right)\delta} \qquad (7)$$

We tried plots of X vs. $\bar{x}$ changing in the values of δ and α, and obtained a curve which coincides with the curve of δ = 2.7 in the inset of Fig. 4 only at the values of δ = 3.0 and α = 0.27. Four points are indicated by red closed circles in the inset. It is known that the percentages of the oxygen gas release, 100α (δ/ (4-2($\bar{x}$)), are 23±1% and those of the nitrogen gas release, 100δ/ (4-2$\bar{x}$), are 84±4% using the relation that $\bar{x}$= 0.14-0.30 for X=12-30%, namely the loss of oxygen is about one fourth of the loss of nitrogen.

Conclusions

In this study, we present a "Slushball Earth" model to explain the occurrence of glaciation and several other geohistorical events. The fact that the evolution of oxygen concentrations up to 400 million years ago, expressed in terms of the mean blockade of ocean-island-type volcanos, $\bar{x}$, and the nitrogen released into the stratosphere while the reservoir was blocked, δ, enhanced the responsibility for the generation of excess oxygen by open system reactions with the blockade of craters at a certain frequency. Ward's data analysis highlighted two important values, δ = 2.7 and $\bar{x}$ = 0.22 ± 0.08 for 12 – 30% oxygen concentrations over 400 million years. A trial model that both the release of nitrogen and oxygen gasses were considered led to the result that δ is not 2.7 but 3.0, and α which represents a release ratio of oxygen to nitrogen is 0.27, that is, the loss of oxygen gas is about one fourth of the loss of nitrogen gas. We excluded H_2O from the atmospheric composition in this study because its form is liquid or solid, but its mass is nearly equal to $\bar{x}O_2$ in Eq. (5). Thus, nuclear transformation is also a strong candidate for the origin of water on Earth.

Authorship contribution statement

Mikio Fukuhara analyzed the data, made all figures and wrote the draft of the manuscript.

Ken'nosuké Hara performed calculations/modeling and edited the paper.

Declaration of competing interes

The authors declare that they have no known competing financial interests or personal relationships that could have appeared to influence the work reported in this paper.

Data availability

All data supporting the findings of this study are available within the article and its supplementary material. All other data are available from the corresponding author upon reasonable request.

Acknowledgements

We would like to thank Editage (www.editage.com) for English language editing.

References

1. Lucht, W. (2011). Revolutions That Made the Earth. Nature, 470(7335), 460-461.
2. Harland, W. B. (1964). Critical evidence for a great infra-Cambrian glaciation. Geologische Rundschau, 54, 45-61.
3. Salyards, S. L., Sieh, K. E., & Kirschvink, J. L. (1992). Paleomagnetic measurement of nonbrittle coseismic deformation across the San Andreas fault at Pallett Creek. Journal of Geophysical Research: Solid Earth, 97(B9), 12457-12470.
4. Hoffman, P.F., Kaufman, A.J., Halverson, G.P., Schrag, D.P (1998) A Neoproterozoic snowball, Science 281:1342-1346.
5. Schopf, J. W., & Klein, C. (Eds.). (1992). The Proterozoic biosphere: a multidisciplinary study. Cambridge University Press.
6. Allen, P. A., & Etienne, J. L. (2008). Sedimentary challenge to snowball Earth. Nature Geoscience, 1(12), 817-825.
7. Fairchild, I. J., & Kennedy, M. J. (2007). Neoproterozoic glaciation in the Earth System. Journal of the Geological Society, 164(5), 895-921.
8. Williams, G. E. (1993). History of the Earth's obliquity. Earth-Science Reviews, 34(1), 1-45.
9. Hara, K. (2009). On the possible reversal of an earth-scale top. Journal of technical physics, 50(4), 375-385.
10. Williams, G. E. (2008). Proterozoic (pre-Ediacaran) glaciation and the high obliquity, low-latitude ice, strong seasonality (HOLIST) hypothesis: Principles and tests. Earth-Science Reviews, 87(3-4), 61-93.
11. Scarborough, J.B. (1958) The Gyroscope, Chs. III, X, Interscience Inc, New York.
12. Jenkins, G. S., & Scotese, C. R. (1998). An early snowball earth?. Science, 282(5394), 1643-1645.
13. Lyons, T. W., & Reinhard, C. T. (2009). Oxygen for heavy-metal fans. Nature, 461(7261), 179-180.
14. Slack, J. F., & Cannon, W. F. (2009). Extraterrestrial demise of banded iron formations 1.85 billion years ago. Geology, 37(11), 1011-1014.
15. Macdonald, F. A., Schmitz, M. D., Crowley, J. L., Roots, C. F., Jones, D. S., Maloof, A. C., ... & Schrag, D. P. (2010). Calibrating the cryogenian. Science, 327(5970), 1241-1243.
16. Donovan, S. K., & Pickerill, R. K. (1997). Dropstones: their origin and significance: a comment. Palaeogeography, Palaeoclimatology, Palaeoecology, 131(1-2), 175-178.
17. Sohl, L. E., Christie-Blick, N., & Kent, D. V. (1999). Paleomagnetic polarity reversals in Marinoan (ca. 600 Ma) glacial deposits of Australia: implications for the duration of low-latitude glaciation in Neoproterozoic time. Geological Society of America Bulletin, 111(8), 1120-1139.
18. Rothman, D. H., Hayes, J. M., & Summons, R. E. (2003). Dynamics of the Neoproterozoic carbon cycle. Proceedings of the National Academy of Sciences, 100(14), 8124-8129.
19. Eyles, N., & Januszczak, N. (2004). 'Zipper-rift': a tectonic model for Neoproterozoic glaciations during the breakup of Rodinia after 750 Ma. Earth-Science Reviews, 65(1-2), 1-73.
20. Peltier, W. R., Tarasov, L., Vettoretti, G., & Solheim, L. P. (2004). Climate dynamics in deep time: Modeling the [snowball bifurcation] and assessing the plausibility of its occurrence. Washington DC American Geophysical Union Geophysical Monograph Series, 146, 107-124.
21. Kasting, J. F. (1993). Earth's early atmosphere. Science, 259(5097), 920-926.
22. Holland, H. D. (2006). The oxygenation of the atmosphere and oceans. Philosophical Transactions of the Royal Society B: Biological Sciences, 361(1470), 903-915.
23. Manning, C.L.M. (2012) National Earth Science Teachers Association, Kentucky Coal Education Web Site. http://www.windows2universe.org/earth/past/oxygen buildup.html.
24. Bates, D. R., & Nicolet, M. (1950). The photochemistry of atmospheric water vapor. Journal of Geophysical Research, 55(3), 301-327.
25. Dutkiewicz, A., Volk, H., George, S. C., Ridley, J., & Buick, R. (2006). Biomarkers from Huronian oil-bearing fluid inclusions: an uncontaminated record of life before the Great Oxidation Event. Geology, 34(6), 437-440.
26. Whitmarsh, J. (1999). The photosynthetic process. Concepts in photobiology.
27. Fukuhara, M. (2020). Did nuclear transformations inside Earth form nitrogen, oxygen, and water?. Journal of Physics Communications, 4(9), 095007.
28. Fukuhara, M. (2014). Nitrogen Discharged from the Earth's Interior Regions. Journal of Modern Physics, 5(2), 75.
29. Honda, S., Yuen, D. A., Balachandar, S., & Reuteler, D. (1993). Three-dimensional instabilities of mantle convection with multiple phase transitions. Science, 259(5099), 1308-1311.
30. Grieve, R. A. (1980). Impact bombardment and its role in proto-continental growth on the early Earth. Precambrian Research, 10(3-4), 217-247.
31. Fukuhara, M. (2022) Earth science and deuterium nuclear reactions: The origins of heat, elements and water, Cambridge Scholars Publishing, Newcastle upon Tyne, UK.
32. Ward, P. (2007) Oxygen – the breath of life, New Sci., Earth. 28: 38. https://www.newscientist.com/article/mg19426012-000-oxygen-the-breath-of -life/
33. Catling, D. C., & Zahnle, K. J. (2009). The planetary air leak. Scientific American, 300(5), 36-43.

Appendix 1

Derivation process and verification method of the graph in Fig. 1

A1-1. Gravity gyroscope-effect

Given a forced directional change, a spinning body moves not into the forced direction, but in the orthogonal direction to the forced change. For example, when a spinning top supported at one end of its axis is released, it resists gravity and circulates horizontally about the vertical axis. This circular motion is a well-known phenomenon, a gyroscopic effect referred to as the gravity gyroscope-effect. The downward gravitational force $\mathbf{F} \propto -\mathbf{k}$ is exactly balanced by an equal and opposite upward force $-\mathbf{F} \propto \mathbf{k}$at the end (pivot); these two forces form a couple which causes a horizontal circular motion, called precession. Two facts holding in this phenomenon are extracted to derive a couple formula in other gyroscope-effects mentioned later, as guiding principles. (1) The magnitude of force in $spin \neq 0$ is the same as that in $spin = 0$, i.e., $\left|\mathbf{F}_{spin\neq 0}\right| = \left|\mathbf{F}_{spin=0}\right|$. (2) The direction of force coincides with the direction of motion in *spin* = 0.

A1-2. Revolution gyroscope-effect by friction

On the other hand, when a gimbal-mounted gyroscope with universal rotational freedom rides on a revolving vehicle (turntable, merry-go-round, etc.) and is put into a retrograde spin, the spin axis inverts vertically and aligns with the vertical axis of revolution. This vertical motion also represents another gyroscopic effect, referred to as the revolution gyroscope-effect. The behavior was once pointed out in 1905 [34] and has been explained dynamically in 2008 [35]. Then, the spin axis resists the revolution and maintains its azimuthal direction at an almost constant. This means that the vehicle revolves at an angular velocity Ω, whereas the top axis spinning at an angular velocity w ($w > \Omega$) circulates at a different angular velocity, i.e., the equal and opposite angular velocity$-\Omega$relative to the floor of the vehicle. A horizontal couple due to friction at the bottom support (pivot or bearing) sustaining the weight of the gyroscope forms a vertical torque, stemmed from the centrifugal force and followed by the guiding principles, which is transmitted to the rotor through gimbals and inverts the spin axis.

The torque formula [35] is obtained as

$$\mathbf{N} = (C - A)\Omega^2 \sin\theta\, \mathbf{e}_3 \times \mathbf{e}_2 \quad , \qquad \text{(A1)}$$

where unit vectors $\mathbf{e}_3$ and $\mathbf{e}_2$ are sown in Fig. A1. Inverting phenomena of a gimbal-mounted gyroscope with universal rotational freedom occur on the center of a turntable or on an orbiting vehicle like merry-go-round. The external torque transmitted from a vehicle to a rotor in an orbiting vehicle results from the force about the center of mass of the rotor, not the force about the center of the circular path. The torque produced by the latter force disappears. Even if *spin* = 0 in the orbital frame at rate Ω ,the top means geometrically to spin at the rate $\omega = \Omega$ relative to an inertial frame, just as Moon orbiting Earth. In this case, the top axis is static relative to the revolution frame and the gyroscope-effect never occurs. The inversion phenomena are only conspicuous when the spin rate w is a little larger than the revolution rate Ω: the smaller the ratio w / Ω (>1), the faster the inversion. When $\omega \gg \Omega$, the inversion phenomena are too slow to observe. Ideally, we should obtain the condition $\omega \cong 1.5 \sim 400\,\Omega$ to observe the inverting phenomena.

Let the spin angular momentum be $\mathbf{L} = Cw\mathbf{e}_3$, then from $d\mathbf{L}/dt = \mathbf{N}$, precession $\dot{\psi}$ and nutation $\dot{\theta}$ are represented as follows to explain the phenomenon quantitatively [35] and provide dynamics in Fig. A2 [37]:

$$\mathbf{e}_2: \quad \dot{\psi} = 0 \qquad (\psi = constant), \qquad \text{(A2)}$$

$$\mathbf{e}_1: \quad \dot{\theta} = -2\beta\Omega\sin\theta \qquad (\cos\theta = \tanh\beta\Omega t), \qquad \text{(A3)}$$

where $$\beta = \frac{C - A}{C}\frac{\Omega}{\omega} \qquad \text{(A4)}$$

and the integral constant is chosen $\cos\theta = 0$ at $t = 0$. Note that the result satisfies the elemental vectorial representation of the gyroscope-effect: $\dot{\boldsymbol{\theta}} \times \mathbf{L} = \mathbf{N}$.

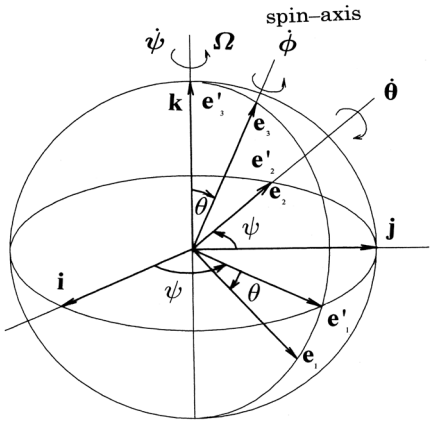

Figure A1: Three reference frames **(i, j, k)** ,($\mathbf{e}'_1$, $\mathbf{e}'_2$, $\mathbf{e}'_3$) , ($\mathbf{e}_1$, $\mathbf{e}_2$, $\mathbf{e}_3$) expressed by unit vectors and three rotational degrees of freedom (ψ, θ, ϕ) (Euler's angles), with the origin at the center of mass of a top: **(i, j, k)** denote an inertial frame; the direction of the spin axis $\mathbf{e}_3$ is represented by (ψ, θ) ; precession (revolution) by $\dot{\boldsymbol{\psi}} = \dot{\psi}\,\mathbf{k} = \dot{\psi}\,\mathbf{e}'_3$ ($\boldsymbol{\Omega} = \Omega\,\mathbf{k}$), nutation by $\dot{\boldsymbol{\theta}} = \dot{\theta}\,\mathbf{e}'_2 = \dot{\theta}\,\mathbf{e}_2$ and spin by $\dot{\boldsymbol{\phi}} = \dot{\phi}\,\mathbf{e}_3$ ($\dot{\phi} = \omega =$ spin rate). The reference frame fixed in the rotor is not used, but C and A are the same as those in $(\mathbf{e}_1, \mathbf{e}_2, \mathbf{e}_3)$ because of axial symmetry.

A1-3. Revolution gyroscope-effect by precession

Orbital planets and satellites have no gimbals to generate friction causing the above type of vertical motion. In *spin* = 0 in the orbital frame ($w = \Omega$ in an inertial frame) just as Moon orbiting Earth, there is no problem: a top axis obeys the revolution to circulate synchronously. But in $spin \neq 0$ ($\omega \neq \Omega$) just as Earth orbiting Sun, there is a problem: Earth revolves around Sun at the rate Ω (360° per year); nonetheless, Earth's axis refuses the revolution $\Omega$and precesses (circulates) at the rate $\dot{\psi}$ (360° per 26000 years). Therefore, riding on a vehicle at the angular velocity Ω , Earth's

axis persists to circulate at the different angular velocity $\dot{\psi}$. Why on earth does the revolution gyroscope-effect occur to align the spin axis with the revolution axis? Hara [36] discussed the possible inversion of the spin axis of a man-made satellite and the search for the ultimate detectable conditions for a realizable experiment. A spinning top in orbit under gravitation is forced to precess around the North Pole normal to the orbital plane. This means that the top's axis circulates at precession rate $\dot{\psi}$ resisting the orbital motion at revolution rate Ω, where it holds $|\dot{\psi}| \ll \Omega$. This resistance may produce a slow revolution gyroscope-effect by precession.

ISS (International Space Station) orbits Earth at the rate Ω (1 revolution per 90 minutes). On Earth's ground, there are many restaurants revolving at the same rate. We need to produce a gimbal-mounted gyroscope spinning at rate w (= 1 rotation per 60 minutes), that is $w = 1.5\Omega$, the same rate as the minute hand of a clock. According to the revolution gyroscope-effect by friction [35], the gimbal-mounted gyroscope must invert in about 7 hours (Fig. A2) [37]. In ISS the same gyroscope may invert in about 11 hours (Fig. A3) [37], according to the revolution gyroscope-effect by precession (Eqs. (A5), (A6)) (hypothesis in [36]). This time scale is a possible experimental time.

Earth's axial tilt is now $\theta = 23.5^{\circ}$ from the Ecliptic North Pole normal to the orbital plane (Ecliptic). Its motion is recognized as a precession (-50 " /year) and nutation (9.2 "/18.6 years). The precession is a retrograde horizontal circular motion with a period equivalent to 360° per 26000 years, and nutation is a vertical reciprocating motion near 23.5°. Vertical one-way motion is never recognized. But, this is based on astronomical observations only in the past several thousand years. This time scale is too short to discuss the history of Earth's axial tilt. However slow it is, one-way motion as the Earth-scale top mentioned later would appear for a long time, perhaps for a million years. Nowadays, if such a revolution gyroscope-effect occurs, it is possible to detect the effect by physical experiments using a man-made satellite.

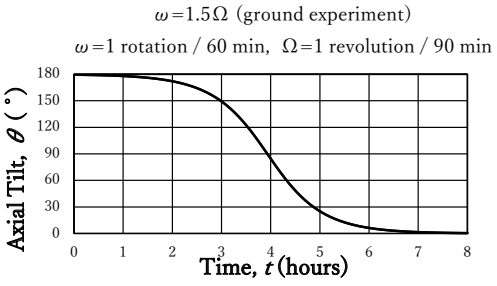

Figure A2: Revolution gyroscope-effect by friction in a restaurant revolving at rate Ω (=1 revolution / 90 min) represents inversion of a gimbal-mounted gyroscope spinning at rate ω (=1 rotation / 60 min). This extremely slow version of gyroscope-effect is necessary to link three different phenomena, that is, ground experiment, satellite experiment, and Earth's axis motion.

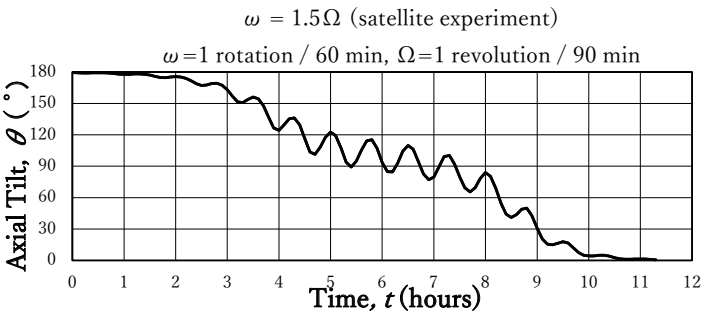

Figure A3: Revolution gyroscope-effect by precession inside ISS revolving at the rate Ω (=1 revolution / 90 min) represents inversion of a gimbal-mounted gyroscope spinning at the rate *w* (=1 rotation / 60 min), in a gravity-free state without friction. Note that the difference in two expected experiments under the same condition. Its realization will prove experimentally the gyroscope-effect by precession. Outstanding nutation waves fade away along with the increase of spin rate ($\omega \geq 10\Omega$) and the curve in the graph becomes smooth like that in Fig. 1 in the text.

A1-4. Dynamics of revolution gyroscope-effect by precession

The dynamics is roughly summarized in two steps as follows (cf. Fig. A1).

(1)Step 1 (dynamics in Fig. A3): Inversion of an orbiting top around Earth with a possible test inside ISS.

The torque produced from Earth's universal gravitation acting at a disc-like top ($C = 2A$) is represented as $\mathbf{N}_{ug} = \frac{3GM}{R^3}\hat{\mathbf{R}} \times \mathbf{I} \cdot \hat{\mathbf{R}}$, where *R* is the distance from

an attracting body to a top, $\hat{\mathbf{R}}$ is its unit vector, and **I** is inertia tensor. Riding on a revolving (Ω) frame, the top's spin axis is forced in a precession motion ($\dot{\psi}$), i.e., a small circulating motion. In other words, a spinning top maintains the slow precession against the quick revolution, therefore the revolution gyroscope-effect by precession may arise and cause rising (inverting) motion ($\dot{\theta} < 0$) to the spin axis. The effect is represented as a hypothetical torque $\mathbf{N}_{rev} = 2(C-A)\Omega|\dot{\psi}|\sin\theta\, \mathbf{e}_3 \times \mathbf{e}_2$, stemmed from Coriolis force and followed by the guiding principles, necessary to be proved by experiment [36]. Let the spin angular momentum be $\mathbf{L} = Cw\mathbf{e}_3$, then from $d\mathbf{L}/dt = \mathbf{N}_{ug} + \mathbf{N}_{rev}$, precession $\dot{\psi}$ and nutation $\dot{\theta}$ are represented as follows:

$$\mathbf{e}_2: \quad \dot{\psi} = -\alpha \cos\theta(1+\cos 2\varphi) \tag{A5}$$

$$\mathbf{e}_1: \quad \dot{\theta} = \alpha \sin\theta \sin 2\varphi - 2\beta|\dot{\psi}|\sin\theta \tag{A6}$$

$$\varphi = \Omega t - \psi \tag{A7}$$

$$\beta = \frac{C-A}{C}\frac{\Omega}{\omega}$$

$$\alpha = \frac{3}{2}\frac{C-A}{C}\frac{1}{\omega}\frac{GM}{R^3} = \frac{3\beta\Omega}{2} \quad \left(\frac{GM}{R^3} = \Omega^2\right),$$

where α expresses the rate-amplitude of the precession and nutation. Eq. (A5) indicates the precession. The first term of the right-hand side of Eq. (A6) represents the nutation (oscillatory) and the second term represents the inversion (accumulative; our new hypothesis). Note that precession resisting revolution becomes a driving force to cause inversion, which acts at the spin axis to align with the revolution axis.

The precession and nutation terms in Eqs (A5) and (A6) are established (e.g., [11, 38]), but the inversion term remains to be proved experimentally. The magnitude-ratio of inversion to nutation in Eq. (A6) is of the order of $\beta|\dot{\psi}|/\alpha \approx |\dot{\psi}|/|\Omega| \ll 1$. In the case of Earth, $|\dot{\psi}|/|\Omega| \cong 1/26000$. The inversion is therefore usually buried in the nutation and difficult to observe. The inversion can be observed, however, using the kinematical difference between the nutation and inversion. Given that the nutation is oscillatory and inversion is one-way, the inversion will ultimately exceed the nutation and emerge over time; in the case of Earth, the time-scale becomes 1 million years.

(2) Step 2 (dynamics in Fig. 1 in the text): Application to Earth's axial tilt

Hara [9] applied this hypothesis to an Earth-scale top, a top modeled after the real Earth, where the effect caused by Moon is more than twice as large as that by Sun. An Earth-scale top is also supposed to be retrograde birth $\theta \sim 180^{\circ}$ and a constant spin rate (1 rotation per 24 hours). Retrograde birth when planetesimals in Keplerian orbits accumulate, is a long-familiar scenario [37]. The spin rate is regarded as constant ever since the birth to single out the influence of the revolution gyroscope-effect by precession.

Discussion followed by Scarborough [11] and Chandrasekhar [38] would be efficient and reliable essentially Then the outline is summarized as follows, where subscripts S and m represent the effects by Sun and Moon, respectively:

$$\dot{\psi} = \dot{\psi}_S + \dot{\psi}_m \qquad \text{(A8)}$$

$$\dot{\psi}_S = -\alpha_S \cos\theta(1+\cos 2\varphi) \qquad (\varphi = \Omega t - \psi) \qquad \text{(A9)}$$

$$\dot{\psi}_m = -\alpha_m \cos\theta(1+\cos 2\varphi_2) \qquad (\varphi_2 = \Omega_2 t - \psi) \qquad \text{(A10)}$$

$$\dot{\theta} = \alpha_S \sin\theta \sin 2\varphi + \alpha_m \sin\theta \sin 2\varphi_2 - 2\beta|\dot{\psi}|\sin\theta \qquad \text{(A11)}$$

$$\alpha_S = \frac{3}{2}\frac{C-A}{C}\frac{1}{\omega}\frac{GM}{R^3} = \frac{3}{2}\frac{C-A}{C}\frac{1}{\omega}\Omega^2 = \frac{3}{2}\beta\Omega$$

$$\alpha_m = \frac{3}{2}\frac{C-A}{C}\frac{1}{\omega}\frac{Gm_2}{r_2^3} = \frac{3}{2}\frac{C-A}{C}\frac{1}{\omega}\frac{\Omega_2^2}{82.5} = \frac{3}{2}\beta\frac{1}{\Omega}\frac{\Omega_2^2}{82.5}$$

where M ($\gg m$), m_2, and m (= 81.5 m_2) are the masses of Sun, Moon, and Earth; R and r_2 are distances from Earth to Sun and Moon, respectively; ω (= 1 rpd), Ω (= 1 rpy), and Ω_2 (= 1/27.32 rpd) denote the spin angular velocity, the revolution angular velocity of Earth around Sun, and the revolution angular velocity of Moon around Earth, respectively; and $t = 0$ is chosen when the direction of Moon is coincident with that of Sun. The only difference from traditional discussion [11, 38] is a hypothetical term $-2\beta|\dot{\psi}|\sin\theta$ in Eq. (A11) to be added anew. For mathematical simplicity, inversion stage is divided into two parts: $\theta \neq 90^{\circ}$; $\theta = 90^{\circ}$.

a) Stage $\theta \neq 90^{\circ}$ (precession-inversion combination) Possibly omitting the periodic terms cos 2 φ, sin 2φ, cos 2φ_2, sin 2φ_2, as each of these terms averages to zero, we have only to treat the average precession $\langle\dot{\psi}\rangle$ and inversion $\langle\dot{\theta}\rangle$ Then the above equations become:

$$\langle\dot{\psi}\rangle = \langle\dot{\psi}_S\rangle + \langle\dot{\psi}_m\rangle = -(\alpha_S + \alpha_m)\cos\theta \qquad \text{(A12)}$$

$$\langle\dot{\theta}\rangle = -2\beta|\langle\dot{\psi}\rangle|\sin\theta = -2\beta|(\alpha_S+\alpha_m)\cos\theta|\sin\theta = -\gamma_0|\sin 2\theta| \qquad \text{(A13)}$$

$$\gamma_0 = \beta(\alpha_S + \alpha_m) \qquad \text{(A14)}$$

Eqs. (A12), (A13) indicate that the precession $|\langle\dot{\psi}\rangle|$ causes the inverting motion $\langle\dot{\theta}\rangle < 0$ and we call this pair a precession-inversion combination. Adopting the $\alpha_S = 17.4''/y$, $\alpha_m = 37.6''/y$ [11, 38], Eqs. (A12) and (A13) become:

$$\langle\dot{\psi}\rangle = -55.0\cos\theta\,(''/y) \quad (= -50.4''/y \quad \text{when} \quad \theta = 23.5^{\circ}), \qquad \text{(A15)}$$

$$\langle\dot{\theta}\rangle = -0.1365|\sin 2\theta|\,(^{\circ}/10^6 \text{ years}). \qquad \text{(A16)}$$

This is a value no longer to be ignored. In studying the inversion of an Earth-scale top, nothing is more important than the time scale perspective, where 10^6 years are taken as a unit of time.

b) Stage θ 90° (nutation-jump)

Eqs. (A8), (A9), (A10), and (A11) become:

$$\dot{\psi} = 0; \quad \dot{\psi}_S = 0 \quad (\psi_s = \text{constant} = \psi_{S90}); \quad \dot{\psi}_m = 0 \quad (\psi_m = \text{constant} = \psi_{m90}), \qquad \text{(A17)}$$

$$\dot{\theta} = \alpha_S \sin 2(\Omega t - \psi_{S90}) + \alpha_m \sin 2(\Omega_2 t - \psi_{m90}) \qquad \text{(A18)}$$

At θ = 90°, the driving power $\dot{\psi}$ (precession) disappears, but instead the nutation vibrates the spin axis to provide the driving power. When the spin axis arrives at the maximum amplitude of oscillation, the spin axis will jump the 90°- barrier . Any time scale of oscillation (nutation) will be negligible in comparison with the time scale of 10^6 years. Thus, we describe the event as the "nutation-jump". Moving into the θ < 90° region, the precession-inversion term revives. Note that it will take an extreme long time to pass through θ ~90° region, compared to the time scale passing the stage θ = 90° region, because $\langle\dot{\theta}\rangle$ in Eq. (A16) becomes extremely small near θ = 90° and elongates time to pass through the 90° - barrier . As a result, a long stay in a sideways tilt $\theta \sim 90^{\circ}$ is compelled. Thus, the Earth-scale top would take a long siesta in the past.

The graph in Fig. 1 in the text indicates a result, starting at present ($\theta = 23.5$) and going back into the past, obtained from

$$\alpha_{\max} \times 1 \text{ year} = 55.0'' = 0.0153^\circ \ (\alpha_{\max} = |\alpha_S + \alpha_m|$$

in Eq.(A15)), as one of five models chosen from among 1.609" and 2.0^O derived from observational and theoretical discussions [9]; 1 million years are appropriated to the nutation-jump. Furthermore, the effect of the tidal friction in slowing down the Earth's spin would elongate the graph into the past. As a result, 4.6×10^6 years ago, the axial tilt at birth might have been smaller less than θ ~179.5^O.

Appendix 2

Formation of N_2, O_2, and H_2O by nuclear transformation

Since it is expected that the formation of nitrogen is distinctively associated with the formation of the carbonaceous rocks, we consider the dynamic reaction that the carbon and oxygen atoms in carbonate crystals interact to form nitrogen atoms. The process comes about as a result of physical catalytic help of excited electrons (e*) arising from plate tectonics and geoneutrinos (ve) [27-29] :

$$^{12}C + {}^{16}O + 2e^* + 2\nu_e \rightarrow 2\ {}^{14}N + {}^{4}He \qquad \text{(A19)}$$

When we reconsider nuclear transmutation under high temperature and pressure, the following reaction is obtained [27-29].

$$^{14}N + {}^{4}He \rightarrow {}^{16}O + {}^{2}D - 3.11 \text{ MeV} \qquad \text{(A20)}$$

Deuteron fusions are generally expressed by the following reactions.

$$^{2}D + {}^{2}D \rightarrow {}^{4}He + \gamma + 23.8 \text{ MeV} \qquad \text{(A21)}$$

and

$$^{2}D + {}^{2}D + {}^{2}D \rightarrow {}^{1}H + {}^{4}He + n + 21.62 \text{ MeV}, \qquad \text{(A22)}$$

where γ and n are the photon and neutron, respectively. From Eqs. (A19), (A21), and (A22), we get

$$^{12}C + {}^{16}O + 2e^* + 2\nu_e + \gamma \rightarrow {}^{14}N + {}^{16}O + {}^{1}H + n - 5.29 \text{ MeV}. \qquad \text{(A23)}$$

Thus Eq. (A23) becomes an important reaction from a viewpoint of geoscience as follows:

$$4\,{}^{12}C + 4\,{}^{16}O + 8e^* + 8\nu_e + 4\gamma \rightarrow 2\,{}^{14}N_2 + 2\,{}^{16}O_2 + 4\,{}^{1}H + 4n$$

$$\rightarrow 2\,{}^{14}N_2\uparrow + {}^{16}O_2\uparrow + 2\,{}^{1}H_2{}^{16}O\uparrow + 4n - 21.16 \text{ MeV}. \qquad \text{(A24)}$$

Eq. (A24) distinctly indicates formation of gases with a N_2 to O_2 to H_2O ratio of 2 : 1 : 2.

References

34. Pickering, W. H. (1905) A little known property of the gyroscope, Nature 71, 608.
35. Hara, K. (2008) Another reversing gyroscope, J. Tech. Phys. 49, 27-37.
36. Hara, K. (2009) On the possible reversal of a satellite spin axis, J. Tech. Phys. 50, 75-85 .
37. Hara, K. (2020) What if a space tippe top comes to be?, NextPublishing Authors Press, Ch.2. ISBN 978-4-8020-9906-6.
38. Chandrasekhar, S. (1995) Newton's Principia for the Common Reader, Oxford University press, Ch.23. ISBN 0-19-852675-X.